Journal of Solid State Chemistry 181 (2008) 1759–1766

Contents lists available at ScienceDirect

Journal of Solid State Chemistry

journal homepage: www.elsevier.com/locate/jssc

Crystal structures and cation ordering of Sr_2AlSbO_6 and Sr_2CoSbO_6

A. Faik [a], M. Gateshki [b], J.M. Igartua [a,*], J.L. Pizarro [c], M. Insausti [d], R. Kaindl [e], A. Grzechnik [f]

[a] Fisika Aplikatua II Saila, Zientzia eta Teknologia Fakultatea, Euskal Herriko Unibertsitatea, P.O. Box 644, Bilbao 48080, Spain
[b] Australian Nuclear Science and Technology Organization, Private Mail Bag 1, Menai, NSW 2234, Australia
[c] Departamento de Mineralogía y Petrología, Facultad de Ciencia y Tecnología, UPV/EHU, PB 644, Bilbao 48080, Spain
[d] Departamento de Química Inorgánica, Facultad de Ciencia y Tecnología, Universidad del País Vasco, Apartado 644, E-48080 Bilbao, Spain
[e] Institute of Mineralogy and Petrology, University of Innsbruck, A-6020 Innsbruck, Austria
[f] Departamento de Física de la Materia Condensada, Facultad de Ciencia y Tecnología, UPV/EHU, PB 644, Bilbao 48080, Spain

ARTICLE INFO

Article history:
Received 19 November 2007
Received in revised form
29 February 2008
Accepted 10 March 2008
Available online 3 April 2008

PACS:
61.10.Nz
61.50.Ks
61.66.Fu
64.70.Kb

Keywords:
Double perovskite
X-ray diffraction
Crystal structure
Phase transitions

ABSTRACT

The two double perovskite oxides Sr_2AlSbO_6 and Sr_2CoSbO_6 were prepared and their structures studied with the X-ray powder diffraction method. At room temperature the crystal structure of Sr_2AlSbO_6 is cubic ($Fm\bar{3}m$), with $a = 5.6058(1)$ Å. It was found that depending on the preparation conditions, the Al^{3+} and Sb^{5+} cations can be either entirely or partially ordered. In the case of the partially ordered Sr_2AlSbO_6 sample, the extension of cation ordering was estimated from the $h\,k\,l$-dependent broadening of the diffraction peaks and the results were interpreted as evidence of the formation of anti-phase domains in the material. Low-temperature Raman spectroscopic measurements demonstrated that the cubic phase of Sr_2AlSbO_6 is stable down to 79 K.

The room-temperature crystal structure of Sr_2CoSbO_6 is trigonal (space group $R\bar{3}$) with $a = 5.6058(1)$ Å and $c = 13.6758(3)$ Å. At 470 K, however, the material undergoes a continuous phase transition and its structure is converted to cubic (space group $Fm\bar{3}m$). The studied Sr_2CoSbO_6 sample was partially ordered, but unlike Sr_2AlSbO_6, no indication of the formation of anti-phase domains was observed.

1. Introduction

In recent years, the structural properties of double perovskite materials with general formula $A_2BB'O_6$ have been extensively studied [1–3]. The double perovskite structure can be represented as a three-dimensional network of alternating BO_6 and $B'O_6$ octahedra, with A-atoms occupying the 12-coordinated interstitial spaces between the octahedra. The aristotype structure of this family is cubic [4] with the space group $Fm\bar{3}m$ (No. 225) [5]. However, due to a mismatch between the size of the A-site cation and the cuboctahedral space between the octahedra, many such materials undergo one [6], two [7], or even more [8] structural phase transitions at different temperatures. These structural transformations can be conveniently described as changes in the way the BO_6 and $B'O_6$ octahedra are rotated with respect to the crystallographic axes of the material to accommodate the size of the A-site cations [9,10]. In previous articles [11–13], we studied the structural phase transitions occurring in the materials with general formula Sr_2BWO_6 and B = Ni,Co,Zn,Ca,Mg,Cd. All of these tungsten oxide materials undergo temperature-induced phase transitions.

The family of strontium antimony oxides with double perovskite structure has attracted considerable attention because of the magnetic properties of some of its members, such as Sr_2FeSbO_6 [14,15]. From structural point of view, different symmetries have been reported for these materials: monoclinic, tetragonal, trigonal, and cubic (Table 1). Despite this variety, very few temperature-dependent structural studies have been conducted [16].

Structural data of previously studied Sr_2MSbO_6 double perovskite oxides are summarized in Table 1. All materials were prepared by solid state reaction method with the exception of the Al-containing material reported in this work for which sol-gel method was also used. The table shows the synthesis temperatures, the tolerance factors [21],

$$t = \frac{r_{Sr} + r_O}{((r_B + r_{B'})/2) + r_O}$$

(calculated using the ionic radii suggested in [22]), the degree of ordering between the M^{3+} and Sb^{5+} cations over the B-sites of the perovskite structure, and the reported symmetry at room temperature. The compound Sr_2MnSbO_6 was not included in the

* Corresponding author. Fax: +34 94 601 3500.
E-mail address: josu.igartua@ehu.es (J.M. Igartua).

0022-4596/$ - see front matter © 2008 Elsevier Inc. All rights reserved.
doi:10.1016/j.jssc.2008.03.029

Table 1
Structural details and preparation conditions of Sr_2MSbO_6 compounds

Compound	Synthesis temperature (K)	Tolerance factor	Degree of ordering (%)	Symmetry at 300 K	Ref.
Sr_2AlSbO_6	1770	1.021	98	$Fm\bar{3}m$	PW
	1375[a]		91	$Fm\bar{3}m$	PW
Sr_2CoSbO_6	1570–1620	1.002	77	$R\bar{3}m$	17
	1770		80	$R\bar{3}$	PW
Sr_2GaSbO_6	1570–1870	0.999	100	Tetragonal	[18]
	–		100	$I4/m$	16
Sr_2FeSbO_6	1570	0.993	80	$P2_1/n$	14
	–		80	$P2_1/n$	15
Sr_2InSbO_6	1470	0.956	100	$P2_1/n$	[19]
Sr_2YSbO_6	1545	0.934	100	$P2_1/n$	[19]
Sr_2HoSbO_6	1670	0.934	100	$P2_1/n$	[20]
Sr_2DySbO_6	1670	0.931	100	$P2_1/n$	[20]

The data shown are as follows: Highest temperature of treatment; tolerance factor calculated from the ionic radii in [22]; experimentally observed degree of cation ordering; symmetry of the crystal structure at room temperature; literature reference. PW stands for present work.
[a] Prepared by sol-gel method.

table because its crystal structure is strongly distorted due to the Jahn–Teller effect [23] and does not follow the trends observed in the other Sr_2MSbO_6 materials. As seen in Table 1, only the Al-containing material reported in this work has a cubic structure at room temperature and a tolerance factor well above 1. Sr_2CoSbO_6 and Sr_2GaSbO_6 are two materials with tolerance factors very close to 1 and with trigonal and tetragonal symmetries, respectively. The rest of the materials are monoclinic and with tolerance factors below 1. The aim of the present work is to analyze the structures and the possible structural phase transitions of Sr_2AlSbO_6 and Sr_2CoSbO_6, as there are no previous studies on the temperature-dependent structural modifications of these materials. This work is a part of a systematic study that we have undertaken on the $AA'BSbO_6$ ($AA' = Ca_2, SrCa, Sr_2$), and (B = Al,Co,Cr,Fe,Sc...) family of materials.

The structure and magnetic properties of Sr_2CoSbO_6 were first studied in [24,25], and it was reported that this material is pseudo-cubic. In addition, it was claimed that this is the first oxide with Co^{3+} being completely in the high-spin ($S = 2$) state, due to the high value found (5.2 μ_B) for the effective magnetic moment. More recently, the room-temperature structure of Sr_2CoSbO_6 (together with $Sr_2CoSbO_{5.63}$) was re-investigated [17], and the suggestion was made that it has a trigonal symmetry with space group $R\bar{3}m$ (No. 166); lattice constants $a = 5.5992(2)$ Å and $c = 13.6609(2)$ Å, and a partial ordering (77%) of the Co^{3+} and Sb^{5+} cations.

Finally, in [26] Sr_2CoSbO_6 was studied using X-ray and neutron powder diffraction methods. It was confirmed that this material is a trigonal perovskite, but due to the lack of cation ordering, the author assigned the $R\bar{3}c$ (No. 167) space group.

It is interesting to note that the assignation of $R\bar{3}m$ space group suggested in [17] is rather unusual for a double perovskite material. The reason is that $R\bar{3}m$ allows the constituent octahedra to be distorted, but not rotated, which is by far the most common modification of the perovskite structure. On the other hand, many trigonal perovskites are reported with $R\bar{3}$ (No. 148) space group which allows out-of-phase rotations of the octahedra around the $[111]_p$ direction of the simple perovskite and corresponds to the ($a^-a^-a^-$) tilt system [9]. The space group $R\bar{3}c$ suggested in [26], corresponds to the ($a^-a^-a^-$) tilt system in the cases of disordered double perovskites and simple perovskites.

These peculiarities of the previous structural determinations warranted a re-investigation of the room-temperature crystal structure of Sr_2CoSbO_6. In a similar re-examination [27] the structure of Ba_2BiSbO_6, which was initially reported to have $R\bar{3}m$ space group, was later shown [28] to be described better by $R\bar{3}$. With respect to Sr_2AlSbO_6, to the best of our knowledge this is the first time that it has been prepared and its room-temperature structure determined.

2. Experimental

2.1. Sample preparation

Sr_2AlSbO_6 (sample 1) was prepared from nanoscale precursors by the following wet-chemical route: 1 mol of Sb_2O_5 was added to a hot aqueous solution of citric acid (in a 1:3 metal–acid relation) and was stirred until the total dissolution of the

$9H_2O$ were dissolved in the same solution and left for 1 h to ensure complexation. The posterior addition of ethyleneglycol ($\frac{3}{4}$ mol of ethylene per 1 mol of citric acid) yielded a more viscous solution, which was dehydrated at 373 K in a sand bath into a gel. This gel was slowly incinerated in a crucible over one day at 723 K in air to eliminate the organic components. Several thermal conditions and various atmospheres were tried until best results were achieved. Two thermal treatments of 10 h at 1223 and 1373 K in air, and one treatment for 10 h at 1373 K in oxygen atmosphere, to assure the oxygen content, yielded the sample of highest purity. The final material has a light-gray color.

Sr_2CoSbO_6 and a second batch of Sr_2AlSbO_6 (sample 2) were prepared by conventional solid state reaction from $SrCO_3$ (99.995%), Sb_2O_5 (99.99%), and $Co(C_5H_7O_2)_3$ (99.99 + %) or Al_2O_3 powders mixed in stoichiometric proportions.

All compounds were used as received from Sigma-Aldrich. The starting materials were mixed and ground in an agate mortar with acetone and subsequently heated in air, in alumina crucibles. The following heat treatment was used: 6 h at 870 K, to eliminate the organic materials; 24 h at 1270 K; 24 h at 1470 K and 24 h at 1670 K; the final sintering was carried out at 1770 K for 72 h. After each heating, the samples were cooled down slowly (3 K/min); and re-ground (re-mixed) to improve homogeneity. In order to control the quality of the obtained material, X-ray diffraction measurements were performed after each heating. No impurity phases were detected neither in the final Sr_2CoSbO_6 material, which has a dark blue color, nor in the Sr_2AlSbO_6 material, which is light-gray as sample 1.

2.2. X-ray powder diffraction measurements

High-quality room-temperature diffraction data were obtained on a Bruker D8 Advance diffractometer equipped with a primary germanium parafocusing monochromator and Bragg–Brentano geometry, using Cu$K\alpha_1 = 1.5406$ Å radiation. A Sol-X energy dispersive detector was used, with a detection window optimized for Cu$K\alpha_1$, in order to avoid the fluorescence radiation from the samples. The data were collected between 15° and 110° in 2θ, with steps of 0.01° (2θ) and a counting time of 10 s per step.

High temperature diffraction data from Sr_2CoSbO_6 were collected on a similar diffractometer, but equipped with a Våntec high speed one-dimensional detector (with 3° of angular aperture), using Cu$K\alpha$ radiation. An Anton Paar HTK2000 high-temperature chamber with direct sample heating (Pt filament) and a temperature stability of 0.5 K was used. The specimens for high temperature measurements were prepared by mixing the material under study with acetone. Then, the mixture was 'painted' over the Pt-strip heater of the evacuated chamber. In order to obtain reliable values for the unit cell parameters at high temperatures, 36 diffraction patterns, covering the 15–120° 2θ interval, were collected between 300 and 650 K, with a temperature step of 10 K. The diffraction peaks from the Pt sample heater that are present in the high temperature diffractograms were excluded from the refinements.

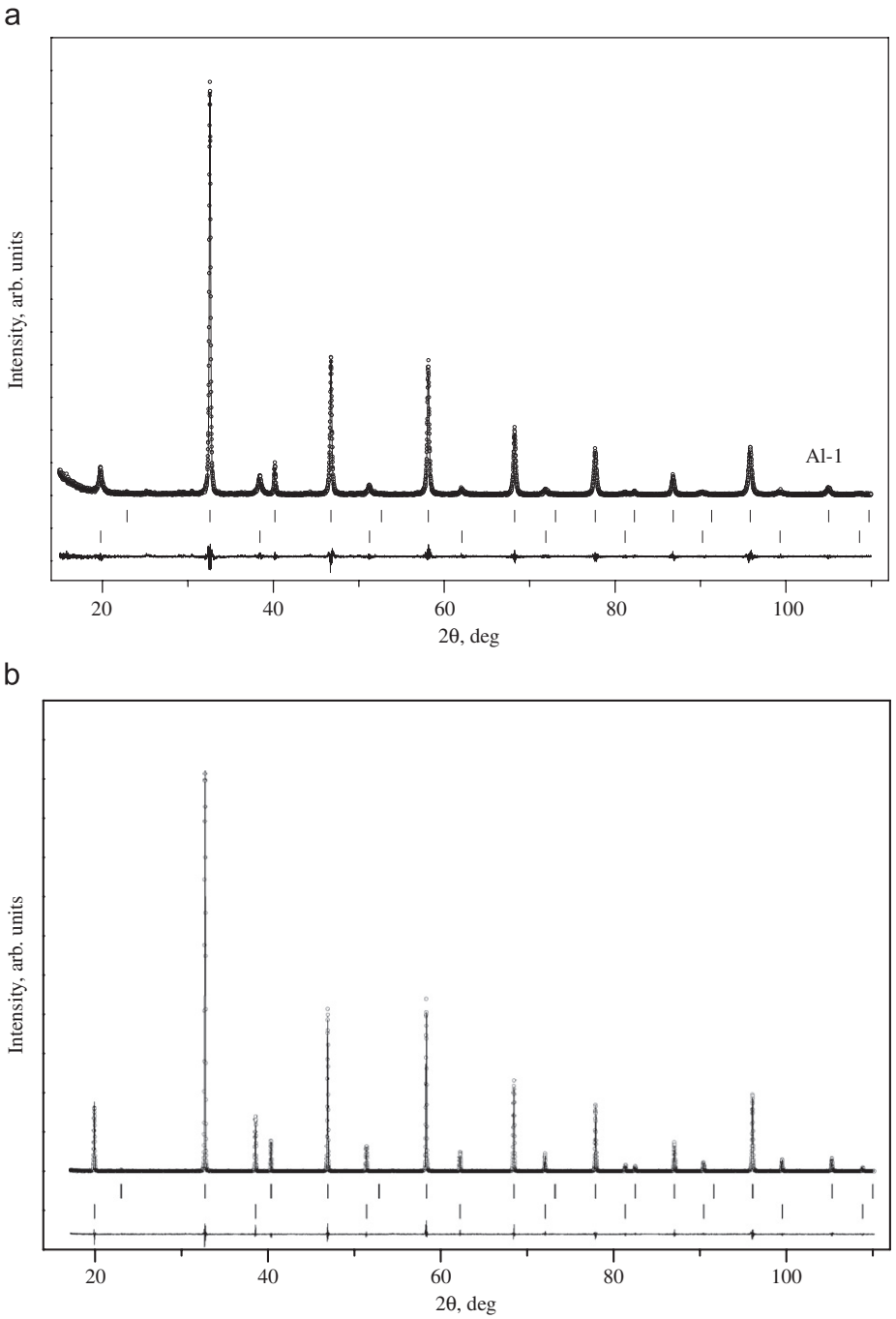

Fig. 1. Experimental (symbols) and calculated (line) powder diffraction profiles for the Rietveld refinement of Sr_2AlSbO_6 at room temperature using a structural model with $Fm\bar{3}m$ space group: (a) sample 1 and (b) sample 2. The bars in the lower part of the graphics represent the Bragg peak positions. The upper set of bars correspond to the simple perovskite structure (sub-cell) and the lower set of bars give the positions of peaks arising from the presence of the B-site cation ordering (super cell).

The Rietveld refinement of the structures was performed using the WinPlotr/FullProf package [29]. The peak shape was described by a pseudo-Voigt function, and the background level was modeled using a polynomial function. The refined parameters were background coefficients, scale factor, lattice constants, atomic positions, independent isotropic atomic displacement parameters, zero shift, peak profile, and asymmetry parameters.

2.3. Raman spectroscopy

Confocal Raman spectra were obtained with a Horiba Jobin Yvon LabRam-HR 800 Raman micro-spectrometer. Samples were excited by the 514.5 and 488.0 nm emission lines of a 30 mW Ar^+-laser and an Olympus 50× objective (N.A. = 0.5). Cooling and temperature control was done with liquid nitrogen and simultaneous heating within a Linkam THMS 600 heating-freezing stage. Sample pellets were placed on the silver block of the stage in a quartz crucible. The temperature inside the crucible was checked by measuring the shift of TO-LO phonon of a polished single crystal Si wafer. Temperature stability during spectra recording and accuracy of temperature measurements was around ±1 °C. The spectra were recorded without polarization filter for the incident laser and the scattered Raman light. Size and power of the laser spot on the surface was approximately 3 μm and 5 mW. The spectral resolution, determined by measuring the Rayleigh line, was about 1.8 cm^{-1}. The dispersed light was collected by a 1024 × 256 open electrode CCD detector. Accuracy of Raman line shifts, calibrated by regular measuring the Rayleigh line, was in the order of 0.5 cm^{-1}.

Table 2
Crystal structure parameters for Sr_2AlSbO_6 (samples 1 and 2) at room temperature

		Sample 1	Sample 2
a (Å)		7.7662(1)	7.7634(1)
Vol (Å^3)		468.40(1)	467.92(1)
O_{1x}		0.252(1)	0.251(1)
B_{iso}(Å^2) Sr		0.64(5)	0.37(4)
B_{iso}(Å^2) Al/Sb		0.22(3)	0.55(3)
B_{iso}(Å^2) O		0.68(7)	0.65(7)
Occupancy	Sb1/Al2(4a)	0.91(1)/0.09(1)	0.98(1)/0.02(1)
	Al1/Sb2(4b)	0.91(1)/0.09(1)	0.98(1)/0.02(1)
R_p (%)		14.1	11.9
R_{Bragg} (%)		3.81	3.31
χ^2		1.93	1.30

The atomic positions are Sr(8c: $\frac{1}{4},\frac{1}{4},\frac{1}{4}$), Sb1/Al2(4a: 0,0,0), Al1/Sb2(4b: $\frac{1}{2},\frac{1}{2},\frac{1}{2}$), O1(24e: $x,0,0$) in the space group $Fm\bar{3}m$.

3. Results and discussion

3.1. Room-temperature structure of Sr_2AlSbO_6 and low-temperature Raman spectroscopy data

X-ray measurements of samples 1 and 2 of Sr_2AlSbO_6 (Figs. 1a and b) revealed that the structure of this material is cubic (undistorted) double perovskite with the $Fm\bar{3}m$ space group.

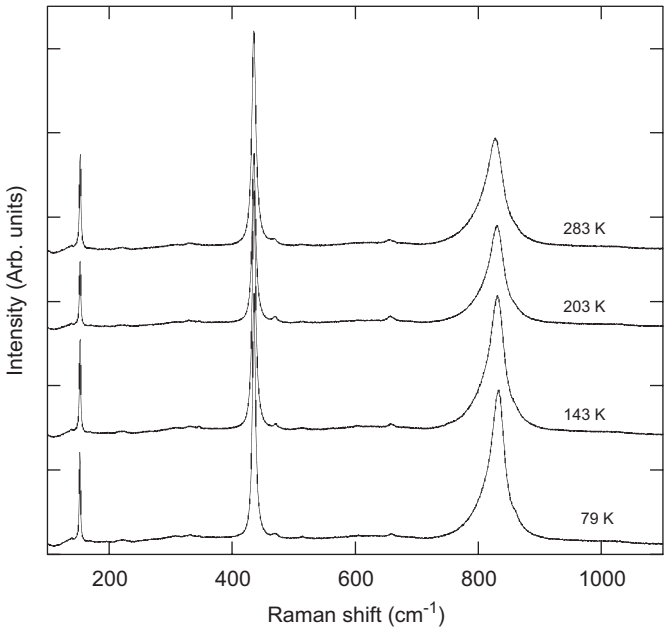

Fig. 3. Raman spectra of Sr_2AlSbO_6 (sample 1) at different temperatures (excitation 514.5 nm). No significant changes are observed at lower temperatures, indicating that the cubic structure observed at 300 K remains stable down to, at least, 79 K.

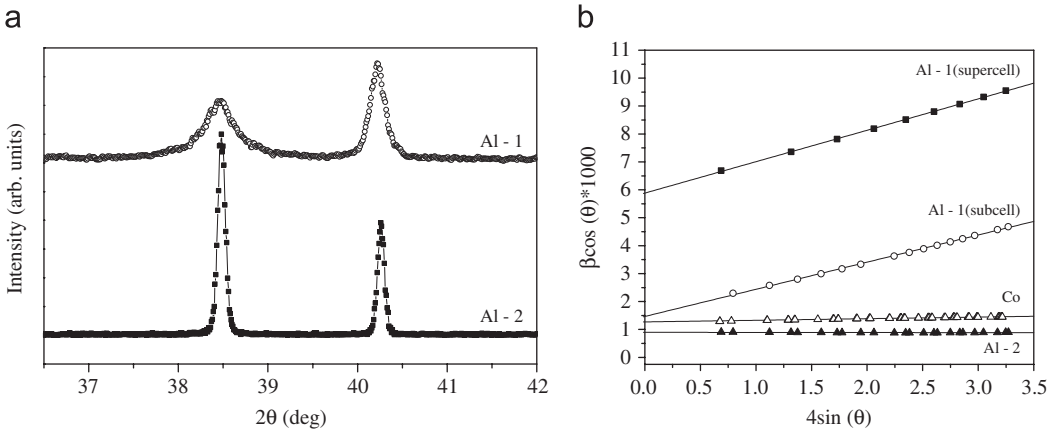

Fig. 2. (a) Comparison between the diffraction data from samples 1 and 2. (b) A Williamson–Hall plot of the diffraction peaks in samples 1 and 2: β denotes the integral breadth corrected for instrumental effects, θ is the diffraction angle. It can be seen that in the case of sample 1 β of the superstructure reflections (solid squares) are clearly larger than those of the rest of the peaks.

Refined structural parameters for the two samples are given in Table 2. Cubic perovskite structures are especially suitable for the study of the degree and the extension of the cation ordering, since in this case the superstructure reflections, i.e. those related to the B-cation ordering, are not overlapping with the order-independent reflections and there is no peak splitting due to unit cell distortion.

Fig. 2 shows a comparison between the diffraction data collected from samples 1 and 2 and a Williamson–Hall plot of the diffraction peaks in the two samples. It can be seen that the superstructure reflections arising from the presence of rock-salt type ordering between the B-site cations (solid squares) are clearly broader than those of the rest of the peaks. From the Rietveld refinement it was obtained that the average crystallite size is about 110 ± 1 nm, and that the effective size of the ordered regions within the crystallites is 17 ± 1 nm. A similar result was obtained in [30] for Sr_2AlTaO_6 and it was interpreted as an evidence for the presence of anti-phase domains. The presence of anti-phase boundaries is also the cause for the increased lattice strain, given by the slope in Fig. 2b. The Rietveld refinement of the diffraction data for sample 1, with variable occupancy factors for the Al and Sb cations, and anisotropic broadening rules accounting for the larger peak widths of the superstructure ($h+k+l=2n+1$) reflections showed that about 91% of the B-cations occupy their respective sites (see Table 2). For sample 2, no hkl specific broadening was observed in the diffraction data and the refined cation ordering was $\approx 98\%$.

It is well known [31] that the degree of cation ordering depends mostly on the charge, size, and polarization properties of the B-site cations. However it can be also affected by the synthesis temperature, sintering time and the method of preparation. In the case of the two Sr_2AlSbO_6 samples discussed here, the difference in the degrees of cation ordering found in samples 1 and 2 is probably related to the methods of preparation and to the sintering temperatures. As mentioned above, samples 1 and 2 were prepared following different routes: sol-gel method with highest temperature treatment at 1373 K and conventional ceramic method with 1770 K.

The Raman spectroscopic measurements of Sr_2AlSbO_6 (sample 2) performed from room temperature down to 79 K are shown in Fig. 3. As seen, there are no notable changes at lower temperatures, and it can be concluded that the cubic structure observed at room temperature remains stable down to, at least, 79 K.

3.2. Room-temperature structure of Sr_2CoSbO_6

The diffraction pattern collected from Sr_2CoSbO_6 at room temperature is shown in Fig. 4. Many diffraction lines are clearly

Table 3
Crystal structure for Sr_2CoSbO_6, at room temperature, in the $R\bar{3}m$ and $R\bar{3}$ space groups

		$R\bar{3}m$	$R\bar{3}$
a (Å)		5.6060(1)	5.6058(1)
c (Å)		13.6762(3)	13.6758(3)
Vol (Å^3)		372.23(1)	372.19(1)
Sr_z		0.2498(3)	0.2499(3)
$O1_x$		0.170(1)	0.128(1)
$O1_y$		−0.170(1)	−0.207(1)
$O1_z$		0.584(1)	0.583(1)
B_{iso}(Å^2) Sr		0.75(5)	0.75(5)
B_{iso}(Å^2) Co/Sb		0.23(5)	0.26(7)
B_{iso}(Å^2) O		2.11(5)	0.88(2)
Occupancy	Sb1/Co2(3b)	0.80(1)/0.20(1)	0.80(1)/0.20(1)
	Co1/Sb2(3a)	0.80(1)/0.20(1)	0.80(1)/0.20(1)
R_p (%)		11.8	8.47
R_{Bragg} (%)		4.28	1.77
χ^2		1.41	1.15

The atomic positions in the $R\bar{3}m$ space group are Sb1/Co2(3b: 0,0,$\frac{1}{2}$), Co1/Sb2(3a: 0,0,0), Sr(6c: 0, 0, z), O1(18h: $x, -x, z$). The atomic positions in the $R\bar{3}$ space group are Sb1/Co2(3b: 0, 0, $\frac{1}{2}$), Co1/Sb2(3a: 0,0,0), Sr (6c: 0, 0, z), O1(18f: x, y, z).

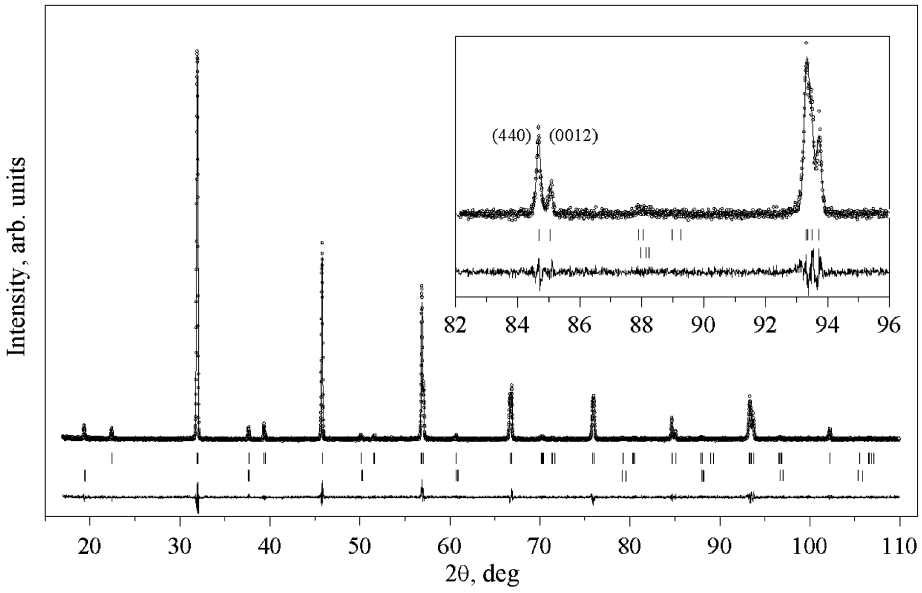

Fig. 4. Experimental (symbols) and calculated (line) powder diffraction profiles for the Rietveld refinement of Sr_2CoSbO_6 at room temperature using a structural model with $R\bar{3}m$ space group. The bars in the lower part of the graphics represent the Bragg peak positions. The upper set of bars correspond to the simple perovskite structure (sub-cell). The lower set of bars give the positions of the superlattice reflections, indicating partial order in the B-site of the double perovskite structure. The inset shows the splitting of the (444) cubic reflection.

split, indicating that the unit cell of this material is not cubic. The observed splitting is consistent with the trigonal symmetry suggested in [17]. For example, the inset in Fig. 4 shows the splitting of the (444) cubic reflection into (440) and (0012) reflections of $R\bar{3}m$.

As a starting model for the Rietveld refinement we used the structure with space group $R\bar{3}m$ suggested in [17]. The results of the refinements are shown in Fig. 4, and the structural details of Sr_2CoSbO_6 at room temperature, refined by assuming the $R\bar{3}m$ space group, are given in Table 3.

It can be seen that the isotropic displacement parameter for the oxygen atoms is larger than the usually observed in similar materials at room temperature (compare with Table 2). The same result was obtained in [17], but no satisfactory explanation was given. Such high isotropic displacement parameters could be an indication that the actual symmetry of the structure is lower than the one used in the refinement. As mentioned above, the most common trigonal space group observed in double perovskite oxides is $R\bar{3}$. As a next step in our study, we attempted a refinement with this space group. The difference between the structural models with $R\bar{3}m$ and $R\bar{3}$ space groups is that in the former the oxygen atoms are located on the plane m $(x, -x, z)$, and in the latter they are allowed to be displaced out of it (see Figs. 5a and b). These two trigonal space groups have the same extinction conditions, and the only way to distinguish between them is to compare the refined structural parameters and agreement factors. The structural details of the room-temperature structure of Sr_2CoSbO_6 refined with the $R\bar{3}$ space group are summarized in Table 3.

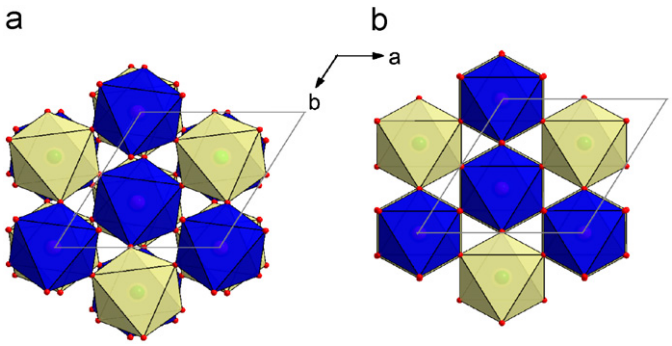

Fig. 5. Projections, along z axis, of the structure of Sr_2CoSbO_6 using the two trigonal models, as indicated. The difference between them is the m mirror plane present in $R\bar{3}m$ and absent in $R\bar{3}$.

Comparing the two structural models shown in Table 3, it can be seen that these models are very similar to each other: the same position ($z = 0.249$) for the Sr^{2+} cation; and very similar values for the isotropic atomic displacements parameters of Co^{3+}, Sb^{5+}, and Sr^{2+} cations. However, it can be also observed that the x and y fractional coordinates of the oxygen atoms are slightly different, and that their isotropic atomic displacement are lower (0.88 Å^2) in the $R\bar{3}$ model compared to the $R\bar{3}m$ model (2.11 Å^2). Also, the refinement with $R\bar{3}$ is both visually (Fig. 6) and statistically (compare agreement factors) better than the one with $R\bar{3}m$. Based on these results, we suggest that the room-temperature structure of Sr_2CoSbO_6 is better described by the $R\bar{3}$ space group, and that the CoO_6 and SbO_6 octahedra are rotated according to the $a^-a^-a^-$ tilt system. Neutron diffraction studies are under way to confirm this result.

The presence of ordering between the Co^{3+} and Sb^{5+} cations is indicated by the superlattice reflections in the room-temperature diffractogram (lower set of reflections in Fig. 4). The degree of this ordering deduced from the final Rietveld refinement in the $R\bar{3}$ space group model is ≈ 80%.

In the case of Sr_2CoSbO_6, despite the high synthesis temperature (1770 K), the degree of ordering is relatively low. This can be explained by the small difference between the radii of the B-site cations: $\Delta r = 0.01$ Å [22]. For comparison, in Sr_2AlSbO_6 this difference is $\Delta r = 0.065$ Å. Another interesting fact is that the sample-related broadening of the diffraction peaks of Sr_2CoSbO_6 does not show any significant $h\,k\,l$ dependence, see Fig. 2b. This suggests that no extended anti-phase boundaries are formed within the crystallites and the observed low degree of ordering is caused by randomly distributed anti-site defects. In the case of trigonal perovskites the effect of the cation ordering on the peak widths cannot be visualized easily as in the case of cubic perovskites (Fig. 2a) due to the overlapping of the order-related reflections with sub-cell reflections (see Fig. 4) and the peak splitting due to the trigonal distortion of the unit cell. The results in this section are based on the independent refinement of the profile parameters of the super-cell and sub-cell reflections.

A remark on the oxygen content of our sample is in order. In [17] it was shown that the oxygen content of the Sr_2CoSbO_6 sample can strongly influence its structure. For example, a sample synthesized in air had about 6% oxygen deficiency and a cubic structure, while a second sample prepared under a high-pressure oxygen atmosphere showed no deficiency and a trigonal structure. Both samples were synthesized using Sb_2O_3 as a source of antimony. In our preparation method no oxygen atmosphere is required to obtain the stoichiometric compounds.

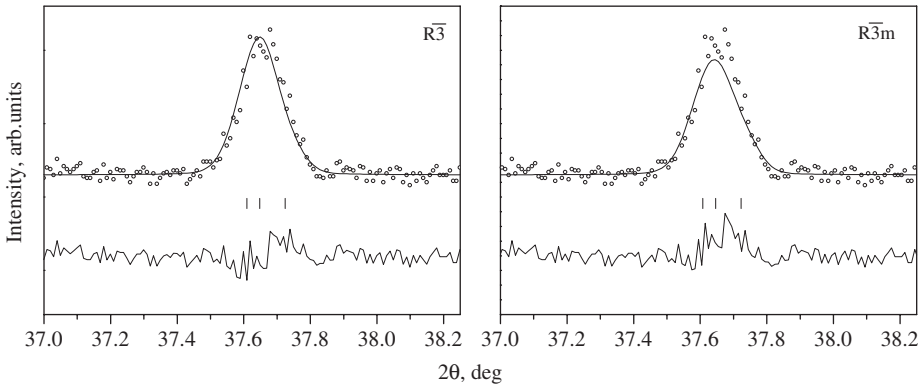

Fig. 6. Rietveld refinement of Sr_2CoSbO_6, at room temperature, using the $R\bar{3}$ and $R\bar{3}m$ space groups. Experimental (symbols) and calculated (line) and difference powder diffraction profiles. The bars represent the Bragg peak positions. The structural model in $R\bar{3}$ fits better the intensity of the peak.

3.3. High-temperature phase transition in Sr_2CoSbO_6

The diffraction patterns collected from Sr_2CoSbO_6 at high temperatures revealed that the peak splitting caused by the trigonal distortion of the unit cell disappears in a continuous way at about 470 K (Fig. 7). This indicates the change of the structure from trigonal to cubic. The patterns collected at temperatures higher than 470 K were well fit by a structural model with the space group $Fm\bar{3}m$, corresponding to the undistorted aristotype double perovskite structure (tilt-system $a^0a^0a^0$). No further changes in the set of observed reflections were found above this temperature, suggesting that the type of unit cell does not change in the temperature range from 470 to 650 K.

Fig. 8 shows the evolution with temperature of the lattice parameters of Sr_2CoSbO_6. In this figure we have represented the unit cell in the rhombohedral description ($a = b = c$, $\alpha = \beta = \gamma$), instead of the hexagonal one ($a = b$, $\gamma = 120^\circ$). This representation is more convenient for observing the disappearance of the trigonal distortion. As it can be observed in Fig. 8, the rhombohedral angle α decreases continuously with the temperature, and at ≈ 470 K it

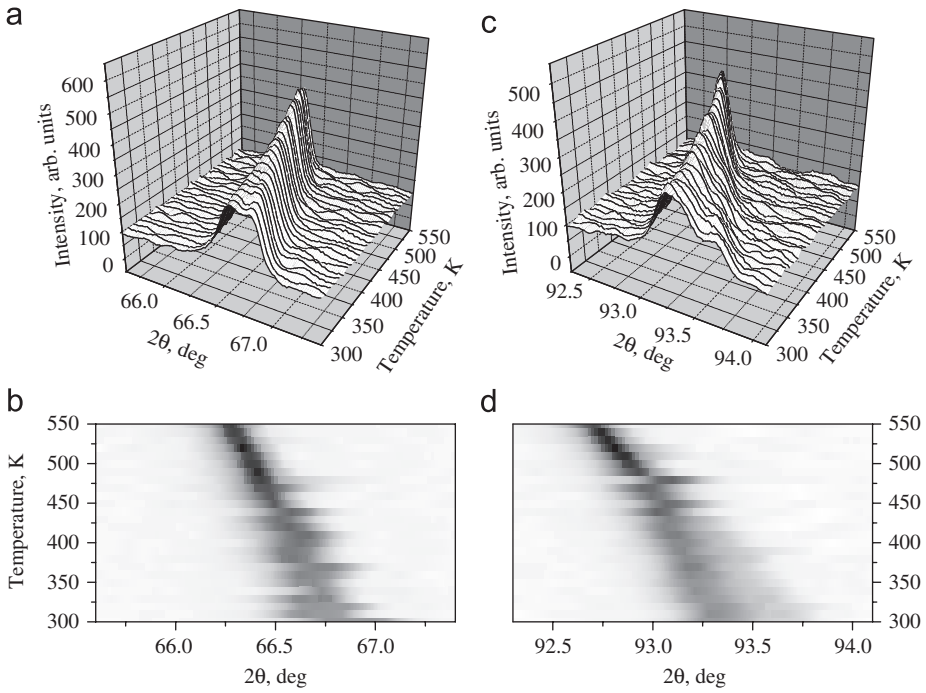

Fig. 7. Thermal evolution of the (440) and (642) cubic reflections, (a) and (c), respectively. In panels (b) and (d) the scattered intensity of the same reflections is projected and represented with shades of gray. Black corresponds to high intensity, and white to low intensity. The trigonal splitting disappears at about 470 K.

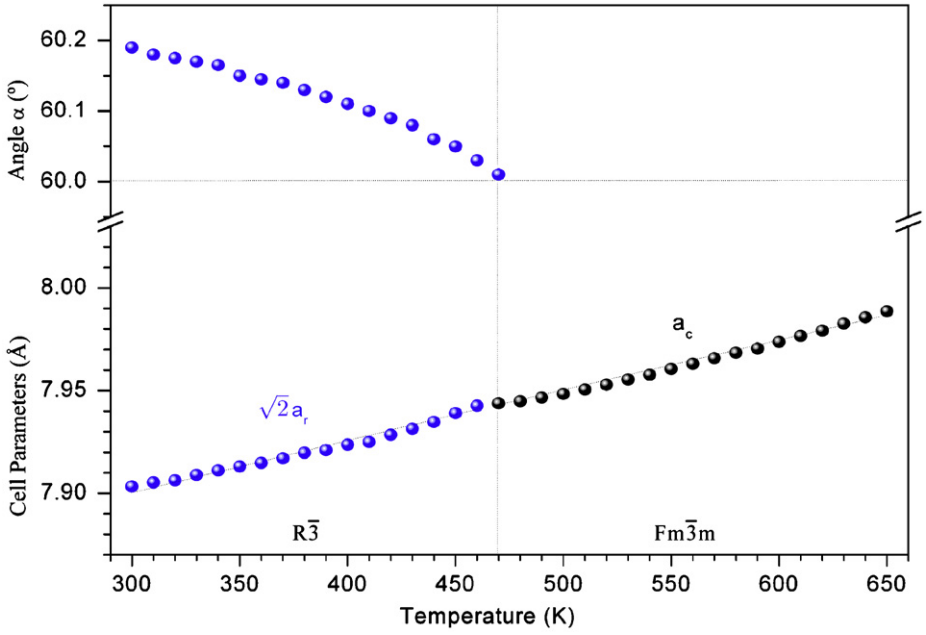

Fig. 8. Temperature evolution of the lattice parameters of Sr_2CoSbO_6 in rhombohedral notation. The rhombohedral angle α decreases continuously with temperature and at ≈ 470 K becomes equal to 60° and the unit cell becomes cubic.

becomes equal to 60°, the value at which the cubic symmetry is attained.

Thus, the structural analysis of Sr_2CoSbO_6 suggests that there is a high-temperature continuous phase transition $R\bar{3} \rightarrow Fm\bar{3}m$ in this compound. Phase transitions of the same type have been observed also in some other double perovskite oxides [32]. The mechanism of these phase transitions related to the mismatch of the size of the A-cation and the cuboctahedral space between the SbO_6 and CoO_6 octahedra. In the particular case of antimony double perovskites the temperature of the phase transition is most likely influenced also by the polarization properties of Sb^{5+}.

It was not possible to perform low-temperature Raman experiments of Sr_2CoSbO_6 due to the high absorption for the used laser wavelengths (514.5 and 488.0 nm). Further studies will be required to establish whether the trigonal structure observed at room temperature is preserved at lower temperatures.

4. Conclusions

The new double perovskite oxide Sr_2AlSbO_6 was prepared and its structure studied with X-ray powder diffraction method. At room temperature the crystal structure of this compound is cubic ($Fm\bar{3}m$) and the performed low-temperature Raman spectroscopic measurements demonstrated that this cubic phase is stable down, to at least, 79 K. Depending on the preparation conditions, the Al^{3+} and Sb^{5+} cations can be either entirely or partially ordered. In the case of the partially ordered Sr_2AlSbO_6 sample, the extension of cation ordering was found to be much smaller than the crystallite size, which suggests the formation of anti-phase domains in the material. At room temperature, the structure of the second compound studied here Sr_2CoSbO_6 was found to be trigonal with space group $R\bar{3}$, which is different from the previously suggested $R\bar{3}m$. The material has partially ordered Co and Sb cations with degree of ordering of $\approx$ 80% deduced from the structural refinement. In this case, however, no evidence of the formation of anti-phase boundaries was found. Sr_2CoSbO_6 undergoes a continuous phase transition at 470 K above which the structure transforms to cubic ($Fm\bar{3}m$).

Acknowledgments

This work was done in part under project nos. UPV 0063.310-13564/2001-2007 and FIS2005-07090.

The authors thank the SGIker General Services of the UPV/EHU, financed by the Programa Nacional de Potenciación de Recursos Humanos del Plan Nacional de Investigación Científica, Desarrollo e Innovación—Ministerio de Ciencia y Tecnología y Fondo Social Europeo (FSE)Ó, for the X-ray diffraction experiments.

References

[1] K.-I. Kobayashi, T. Kimura, H. Sawada, K. Terakura, Y. Tokura, Nature 395 (1998) 677–680.
[2] M. DeMarco, H.A. Blackstead, J.D. Dow, M.K. Wu, D.Y. Chen, E.Z. Chien, H. Haka, S. Toorongian, J. Fridmann, Phys. Rev. B 62 (2000) 14301–14303.
[3] Y. Todate, J. Phys. Chem. Solids B 60 (1999) 1173.
[4] P.M. Woodward, Acta Cryst. B 53 (1997) 32.
[5] T. Hahn (Ed.), International Tables for Crystallography, vol. A, Kluwer, Dordrecht, 2002.
[6] O. Chmaissem, R. Kruk, B. Dabrowski, D.E. Brown, X. Xiong, S. Kolesnik, J.D. Jorgensen, C.W. Kimball, Phys. Rev. B 62 (2000) 14197.
[7] K. Yamamura, M. Wakeshima, Y. Hinatsu, J. Solid State Chem. 179 (2006) 605–612.
[8] L.O. Martin, J.P. Chapman, E. Hernndez-Bocanegra, M. Insausti, M.I. Arriortua, T. Rojo, J. Phys. Condens. Matter 16 (2004) 3879–3888.
[9] A.M. Glazer, Acta Cryst. B 28 (1972) 3384;
A.M. Glazer, Acta Cryst. A 31 (1975) 756–762.
[10] C.J. Howard, B.J. Kennedy, P.M. Woodward, Acta Cryst. B 59 (2003) 463–471.
[11] M. Gateshki, J.M. Igartua, E. Hernández-Bocanegra, J. Phys. Condens. Matter 15 (2003) 6199–6217.
[12] M. Gateshki, J.M. Igartua, J. Phys. Condens. Matter 16 (2004) 6639–6649.
[13] M. Gateshki, J.M. Igartua, A. Faik, J. Solid State Chem. 180 (2007) 2248–2255.
[14] E.J. Cussen, J.F. Vente, P.D. Battle, T.C. Gibb, J. Mater. Chem. 7 (1997) 459–463.
[15] N. Kashima, K. Inoue, T. Wada, Y. Yamaguchi, Appl. Phys. A 74 (2002) S805–S807.
[16] M.W. Lufaso, R.B. Macquart, Y. Lee, T. Vogt, H.C. Loye, J. Phys. Condens. Matter 18 (2006) 8761–8780.
[17] V. Primo-Martín, M. Jansen, J. Solid State Chem. 157 (2001) 76–85.
[18] A. Tauber, S.C. Tidow, R.D. Finnegan, W.D. Wilber, Physica C 256 (1996) 340–344.
[19] W.T. Fu, D.J.W. Ijdo, Solid State Commun. 134 (2005) 177–181.
[20] H. Karunadasa, Q. Huang, B.G. Ueland, P. Schiffer, R.J. Cava, Proc. Natl. Acad. Sci. V 100 (2003) 8097–8102.
[21] V.M. Goldschmidt, Str. Nor. Vidensk. Akad. Oslo 1 (1926) 1.
[22] R.D. Shannon, Acta Cryst. A 32 (1976) 751.
[23] M. Lufaso, P.M. Woodward, J. Goldberger, J. Solid State Chem. 177 (2004) 1651–1659.
[24] G. Blasse, J. Inor. Nucl. Chem. 27 (1965) 993.
[25] G. Blasse, J. Appl. Phys. 36 (1965) 879.
[26] P.W. Barnes, Exploring structural changes and distortions in quaternary perovskites and defect pyrochlores using powder diffraction techniques, Ph.D. Dissertation, The Ohio State University, 2003, ⟨http://www.ohiolink.edu/etd/view.cgi?osu1064346592⟩.
[27] W.T. Fu, R. deGelder, R.A.G. Graaff, Mater. Res. Bull. 32 (1997) 657–662.
[28] W.T. Fu, Solid State Commun. 116 (2000) 461–464.
[29] J. Rodríguez-Carvajal, Physica B 192 (1993) 55–69.
[30] P.M. Woodward, R.D. Hoffmann, A.W. Sleight, J. Mater. Res. 9 (1994) 2118–2127.
[31] M.T. Anderson, K.B. Greenwood, G.A. Taylor, K.R. Poeppelmeier, Prog. Solid State Chem. 22 (1993) 197–233.
[32] R.H. Mitchell, Perovskites. Modern and Ancient, Almaz Press, 2002.